ISSN 1027-5495. Functional Materials, 29, No.4 (2022), p. 514-520.
doi:https://doi.org/10.15407/fm29.04.514

Study of properties of AlB_{12}–Al electric spark coatings on Steel 45

***A.P.Umanskyi*[1], *A.I.Dukhota*[2], *V.E.Sheludko*[1], *V.B.Muratov*[1], *V.V.Kremenitsky*[3], *I.S.Martsenyuk*[1], *M.A.Vasilkovskaya*[1], *A.D.Kostenko*[1], *D.S.Kamenskyh*[4]**

[1]Frantsevich Institute for Problems of Materials Science, National Academy of Sciences of Ukraine, 3 Krzhyzhanovsky Str., 03142 Kyiv, Ukraine
[2]National Aviation University, Aerospace Faculty, 1 Liubomyra Huzara Ave., 03058 Kyiv, Ukraine
[3]Technical Center, National Academy of Sciences of Ukraine, 13 Pokrovskaya Str., 04070 Kyiv, Ukraine
[4]V.P.Kukhar Institute of Bioorganic Chemistry and Petrochemistry, National Academy of Sciences of Ukraine, 50 Kharkovskoe Shausse, 02160 Kyiv, Ukraine

Received June, 23, 2022

The article deals with the study of the structure and properties of electric spark coatings of AlB_{12}-50 wt.% Al aluminum-matrix composite electrode material on Steel 45. The fundamental possibility of obtaining such coatings is estimated by theoretical calculation of the Palatnik criterion (0.11). The thermal conductivity coefficient and heat capacity of the composite were calculated or determined experimentally. The kinetics of mass transfer during electrospark alloying (ESA) has been studied. Taking into account rather high values of the cathode mass increase, the coating deposited in 4 mode (E = 0.61 J, τ = 170 μs) of the ALIER-52 setup was selected for further research. The thickness (h ~ 53 μm), microhardness (H_μ = 10 GPa) and dry friction wear 5.01 mg/(km·cm^2) were determined for the coating. The phase composition of the coating was studied with a Rigaku MiniFlex 300/600 diffractometer; elemental X-ray spectrum analysis of the surface and cross-section was carried out using a JEOL JSM-6490 LV scanning electron microscope with energy-dispersive X-ray microanalysis. $Al_{13}Fe_4$, $AlFeO_3$, AlB_2 and Al_2O_3 phases and small quantities of Al, B, B_2O_3, $AlBO_3$, AlFe, $AlFe_3$ and AlB_{10} were revealed in the coating by X-ray analysis. The wear of ESA-coated specimens was 2.7 times less than that of an uncoated one. A conclusion is made about the possibility of using this electrode material for ESA coatings of steels.

Keywords: AlB_{12}–Al composite, ESA, mass transfer kinetics, structure, phase composition, microhardness, wear.

Дослідження властивостей електроіскрових покриттів AlB_{12}–Al на сталі 45. *О.П.Уманський, О.І.Духота, В.Є.Шелудько, В.Б.Муратов, В.В.Кременицький, І.С.Марценюк, М.А.Васильківська, О.Д.Костенко, Д.С.Каменських*

Статтю присвячено дослідженню структури та властивостей електроіскрових покриттів з алюмоматричного композиційного матеріалу AlB_{12}-50 мас.% Al на сталі 45. Оцінено теоретичну можливість отримання таких покриттів за допомогою теоретичного розрахунку критерію Палатніка (0,11). Коефіцієнт теплопровідності та теплоємність композиту були розраховані чи визначені експериментально. Досліджено кінетику

масопереносу під час електроіскрового легування (ЕІЛ). Зважаючи на достатньо високі значення приросту катоду, для подальшого дослідження обрано покриття, що нанесене на 4 режимі (E = 0,61 Дж, τ = 170 мкс) установки ALIER-52. Для нього визначено: товщина (h ~ 53 мкм), мікротвердість (H_μ = 10 ГПа) та знос при сухому терті 5,01 мг/(км·см^2). Фазовий склад покриття вивчено за допомогою дифрактометра Rigaku MiniFlex 300/600, а елементний рентгеноспектральний аналіз поверхні та поперечного перерізу проведено на скануючому електронному мікроскопі JEOL JSM-6490 LV, обладнаному системою енергодисперсійного рентгенівського мікроаналізу РФА. В покритті виявлено $Al_{13}Fe_4$, $AlFeO_3$, AlB_2 та Al_2O_3, а також сліди Al, B, B_2O_3, $AlBO_3$, AlFe, $AlFe_3$ и AlB_{10}. Показано, що знос зразку з ЕІЛ покриттям у 2,7 рази менший, ніж зразку без покриття. Зроблено висновок про перспективність застосування даного електродного матеріалу для ЕІЛ покриття сталей.

1. Introduction

It is known [1] that up to 70 % of machine parts and technological equipment fail as a result of natural wear. To increase the wear resistance, protective coatings applied to the working surfaces of parts are quite effective [1–5]. For this, various technologies are used, for example, concentrated energy flows. One of them is the method of electrospark alloying (ESA) [6], in which the anode material eroded by a spark discharge is transferred and deposited on the surface of a workpiece (cathode), forming a hardened layer with improved physical and mechanical properties. Various refractory compounds, namely carbides, nitrides, aluminides, silicides, and borides can be used as the anode material [7–9]. Among the latter, aluminum dodecaboride AlB_{12} is of interest. The method of its synthesis from Al and BN developed at the Frantsevich Institute for Problems of Materials Science of NAS of Ukraine, turned to be more rational and cost-effective than direct synthesis from Al and B [10]. AlB_{12} has a low density (~2.52 g/cm^3), and the particularity of its crystalline structure (icosahedral boron framework) determines its high hardness (22–24 GPa), and refractoriness (2070°C) [11].

However, the low crack resistance of aluminum dodecaboride significantly limits the scope of its application [11]; therefore, it is advisable to use AlB_{12} in combination with ductile bonded metal. It is promising to use aluminum, which is characterized by high plasticity, low density (2.7 g/cm^3) and low melting point (660°C). Previously, it was found that Al wets AlB_{12} well with the formation of contact angles ($\Theta \approx 20$ deg), and there are no secondary phases in the interaction zone at the Al–AlB_{12} interface [11]. In addition, aluminum, which has a resistivity of 2.7 μΩ·cm, acts as a kind of additive increasing the conductivity of the AlB_{12}–Al composite (a resistivity of AlB_{12} — 10^6 Ω · cm), which is of great importance in ESA.

The aim of the work is to investigate the possibility of using the composite material "AlB_{12}–Al" to obtain ESA-coatings on Steel 45, and to study the properties of these coatings.

2. Experimental

The AlB_{12} samples were prepared from the powder synthesized at the IPMS of NASU according to the procedure described in [12, 13]. At first, a porous AlB_{12} ceramic frame was obtained. Then it was impregnated with Al melt in vacuum ($1.33 \cdot 10^{-4}$ Pa) at a temperature of ~ 1100°C. This made it possible to obtain an aluminum-matrix composite of AlB_{12}-50 wt.% Al in the form of a bar of 50×50×5 mm in size, from which the electrodes for ESA were cut by the electro-erosion method.

Fig. 1 shows the electrode material AlB_{12}-50 wt% Al microstructure obtained with a

Table 1. Chemical composition of the composite material AlB_{12}-50 wt.% Al (Fig. 1, inset)

Spectrum	Element, wt.%						Total
	B	C	N	O	Al	Fe	
1	82.07	0.66	–	0.03	16.92	0.32	100.00
2	81.52	0.88	0.15	0.05	17.00	0.40	100.00
3	78.77	3.94	1.01	0.45	15.83	–	100.00
4	0.26	0.60	0.67	47.02	51.45	–	100.00
5	1.37	1.97	0.11	1.81	94.74	–	100.00

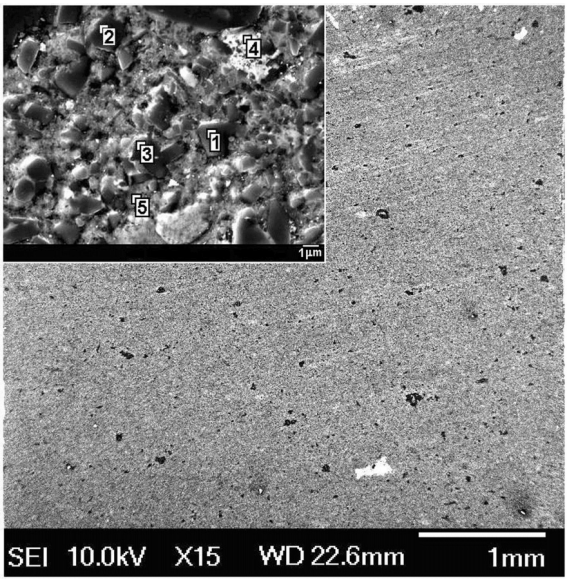

Fig. 1. Microstructure of the cross-section of the electrode material AlB_{12}-50 wt.% Al (inset — enlarged fragment with elemental analysis data).

JEOL JAMP9500F microanalyzer. The material consists of three phases: a metal matrix, AlB_{12} grains (the size of which varies in the range of 1–4 μm) uniformly distributed in the matrix, and Al_2O_3 particles (Fig. 1, inset).

The chemical composition of the main phases of the AlB_{12}-50 wt.% Al composite was determined by X-ray spectral microanalysis (Table 1).

ESA processing of samples (Steel 45, GOST 1050-88) of 1×1 cm in size was carried out on an ALIER-52 installation (SCINTI, Chisinau, RM) at the modes indicated in Table 2. For each minute of the processing of 1 cm^2 of the sample surface, the specific erosion of the anode (Δa) and specific gain in the cathode mass (Δk) were measured with an accuracy of 10^{-4} g on an electronic balance OHAUS Adventurer AR0640. The total anode erosion ($\Sigma\Delta a$), gain in the cathode mass ($\Sigma\Delta k$), and the average mass transfer coefficient $K' = \Sigma\Delta k/\Sigma\Delta a$ were calculated during the alloying time $\tau =$ 10 min/cm^2.

The density of the electrode material was determined by the method of hydrostatic weighing (GOST 25281-82). Heat capacity was measured by the calorimetric method (GOST 23250-78). Thermal conductivity coefficient was obtained according to the method described in [14]. The microhardness of the coatings was measured on a PMT-3 microhardness tester at a load of P = 0.5 N. Tribotechnical studies of the coatings were carried out on a MT-68 friction machine according to the pin-on-disk scheme in the mode: P = 0.2 MPa, V = 4 m/s, friction path S = 3 km. Hardened U8 steel (HRC 61-63) was used as a counterbody.

Table 2. Technological parameters of the ALIER-52 installation

Mode	Pulse duration, μs ± 20 %	Pulse current amplitude value, A ± 20 %	Pulse energy, E, J
2	40	125	0.09
4	170	200	0.61
6	700	200	2.52

X-ray analysis of the coating surface was carried out on a MiniFlex 300/600 diffractometer (Rigaku Corp., Tokyo, Japan) in CuK_α filtered radiation (λ = 1.5418 Å). The structure of the coatings was studied using a JEOL JSM-6490 LV scanning electron microscope equipped with system of energy-dispersive X-ray microanalysis (Oxford Instruments plc.).

3. Results and discussion

Theoretically, the interaction between the electrode and the substrate can be estimated and, to some extent, the composition of the coating can be predicted using the Palatnik criterion [15, 16], which relates only the physical constants of the electrode materials as follows:

$$\frac{\tau_a}{\tau_c} \cong \frac{c_a\rho_a\lambda_a(T_a - T_0)^2}{c_c\rho_c\lambda_c(T_c - T_0)^2}$$

where (for the anode and cathode, respectively) τ_a and τ_c are the characteristic times of erosion (formation of melting centers in the discharge zone); $c_{a,c}$ is the heat capacity, J/(kg·K); $\rho_{a,c}$ is the density, kg/m^3; $\lambda_{a,c}$ is the coefficient of thermal conductivity, W/(m·K); $T_{a,c}$ is the melting point, K; T_0 is the ambient temperature.

This ratio does not take into account a large number of factors affecting the ESA process, but, it can be used for a quantitative evaluation of 3 types of interactions between the anode and cathode made of various materials, namely:

— at $\tau_a << \tau_c$ a coating is formed on a cathode surface;

— at $\tau_a \sim \tau_c$ a coating can be formed as an anode-cathode alloy;

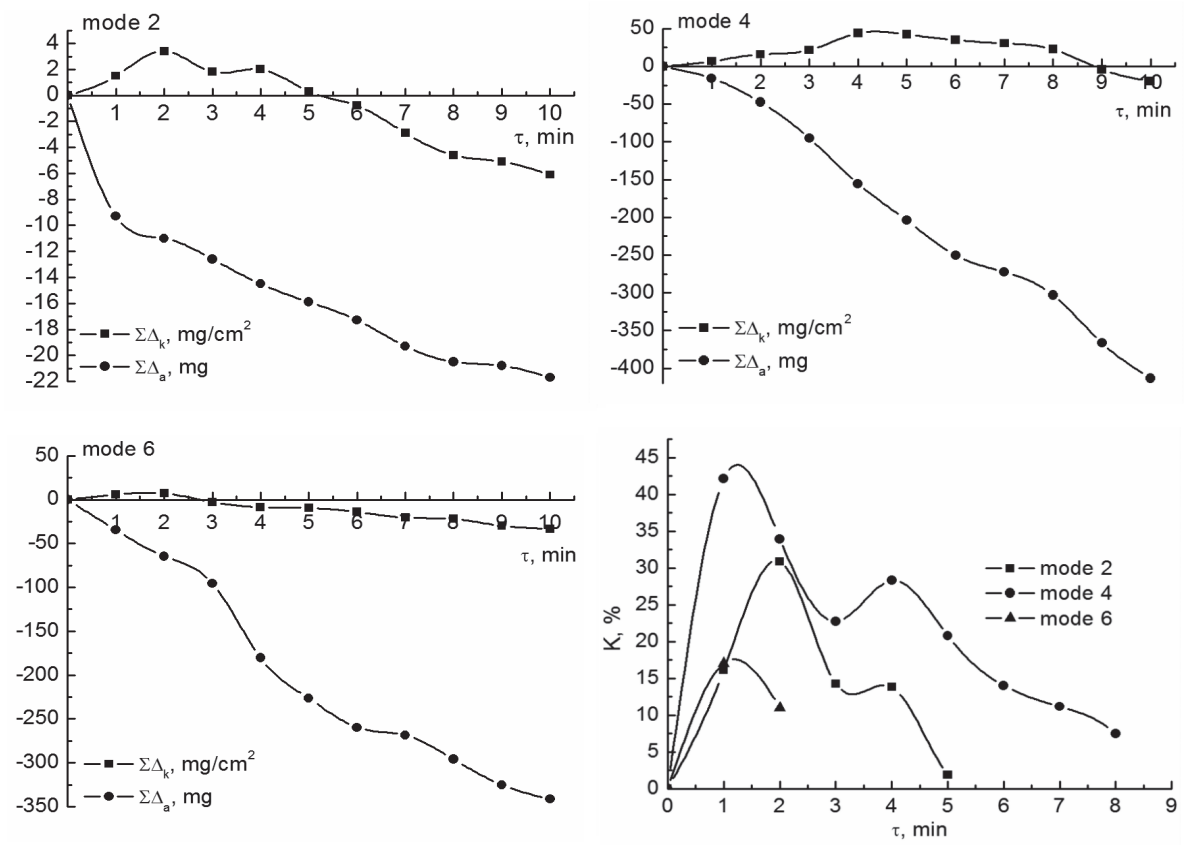

Fig. 2. Kinetic dependences of the total cathode mass gain $\Sigma\Delta k$, the total anode erosion $\Sigma\Delta a$, and the average value of the mass transfer coefficient K' at ESA of 1 cm^2 of Steel 45.

— at $\tau_a >> \tau_c$, no material transfer from anode to cathode, but the transfer of material from cathode to anode is possible [15, 16].

The data required for calculations according to the Palatnik criterion under our conditions are given in Table 3.

It follows from the calculations that ESA coating of AlB_{12}-50 wt.% Al on a Steel 45 substrate can be obtained.

Fig. 2 shows the kinetic dependences of the total anode erosion and the cathode mass gain. These data indicate that at the pulse energy of $E = 0.09$ J (mode 2), for 2 min of alloying we obtain $\Sigma\Delta k = 3.4$ mg/cm^2 and $\Sigma\Delta a = 11$ mg. The negative gain in the mass of the cathode Δk was recorded for the first time for 3 min (i.e., the threshold of the brittle destruction of the doped layer is $T_x = 3$). The average coefficient of mass transfer K' is 30.9 % for 2 min.

With an increase in the pulse energy to $E = 0.61$ J (mode 4), $\Sigma\Delta k = 44$ mg/cm^2, $\Sigma\Delta a = 155.4$ mg for 4 min of alloying. Under these conditions, K' is 42.13 % for

Table 3. Physical characteristics of the electrode materials and the value of the Palatnik criterion

Characteristics	Anode (AlB_{12}-50 wt.% Al)	Cathode (Steel 45) [17, 18]	The value of the Palatnik criterion τ_a/τ_c
λ, W/(m·K)	72.58	79	0.11
C_p, J/(kg·K)	918.88	473	
T_m, K	933*	1763**	
ρ, kg/m^3	2616	7826	

* T_m of the most low-melting phase (Al) was used for the calculation
** Calculation by [19]

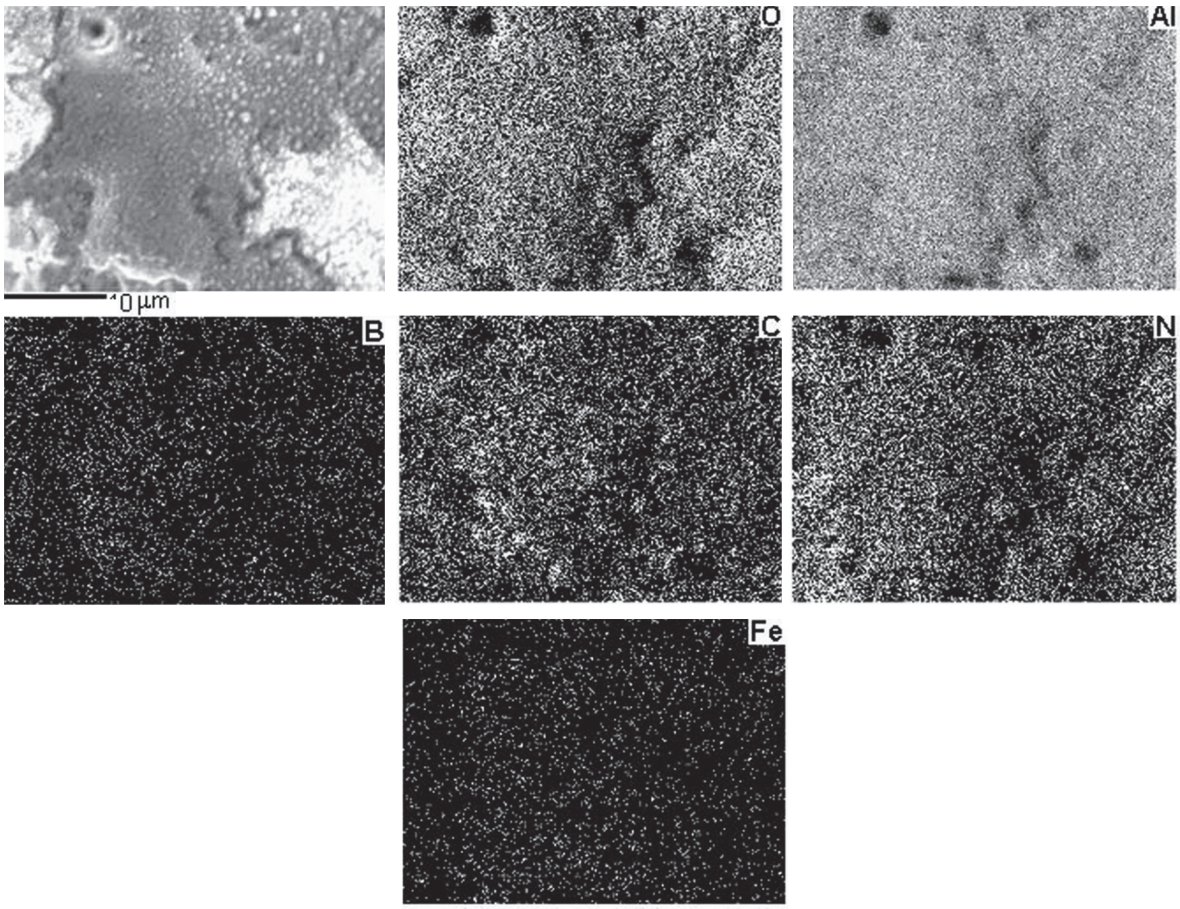

Fig. 3. Microstructure of the surface of a ESA coating AlB_{12}-50 wt.% Al on Steel 45 with distribution of the elements according to X-ray microanalysis.

1 min of the treatment with a decrease to 28.3 % for 4 min, $T_x = 5$.

The 6 mode ($E = 2.52$ J) is characterized by the values of $\Sigma\Delta k = 7.1$ mg/cm^2 and $\Sigma\Delta a = 64.5$ mg for 2 min of treatment. $K' = 17.05$ % for 1 min, followed by a decrease to 11 % for 2 min, $T_x = 3$.

The mode 4 (compared to the modes 2 and 6) is characterized by rather high values of $\Sigma\Delta k$ and K' in the first minutes of alloying, and the coating applied in the mode was chosen for further research. The microstructure of the fused surface of ESA coating applied in the 4 mode is shown in Fig. 3. It should be noted that the Al content is high (from 53 to 64.46 wt.%). In addition, the surface layer contains: O — from 7 to 17 wt.%, C — from 7 to 14 wt.%, N — from 6 to 13 wt.%, Fe — from 8 to 12 wt.%. Boron is evenly distributed over the entire surface.

The coating is multiphase: X-ray analysis showed the presence of main phases $Al_{13}Fe_4$, $AlFeO_3$, AlB_2, Al_2O_3, and small quantities of Al, B, B_2O_3, $AlBO_3$, AlFe, $AlFe_3$, and AlB_{10} (Fig. 4). The absence of the AlB_{12} phase is noteworthy. The ESA process occurring at plasma temperatures ($2\cdot10^4$ K) in air is known to be accompanied by thermo-oxidative destruction of anode and cathode materials [20]. Such harsh conditions contribute to the destruction of aluminum dodecaboride into its constituent elements at $T = 2300$ K [21]. Oxidation of AlB_{12} (at $T = 1273$ K) can also occur with the formation of boron oxide B_2O_3 and aluminum borate $9Al_2O_3{\cdot}2B_2O_3$ [22], as well as oxidation of AlB_{10} (at $T \sim 973$ K) — with the formation of $2Al_2O_3{\cdot}B_2O_3$ [23]. The formation of the AlFe and $AlFe_3$ phases during the deposition of ESA coatings was also noted earlier [24–26]. The most characteristic phase in the coating is the intermetallic compound $Al_{13}Fe_4$ located at a depth of ~ 5 μm from the surface in the form of a layer of dark stripes of ~ 20 μm wide (Fig. 5, spectra 3 and 5, Table 4). These data correlate, to some extent, with the data of [27], which

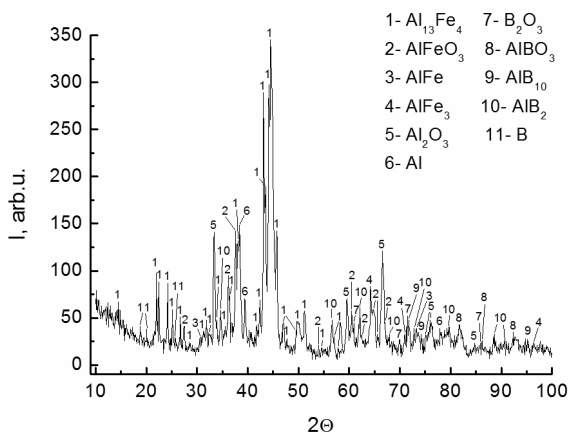

Fig. 4. Diffraction pattern of a ESA coating AlB_{12}-50 wt.% Al on Steel 45.

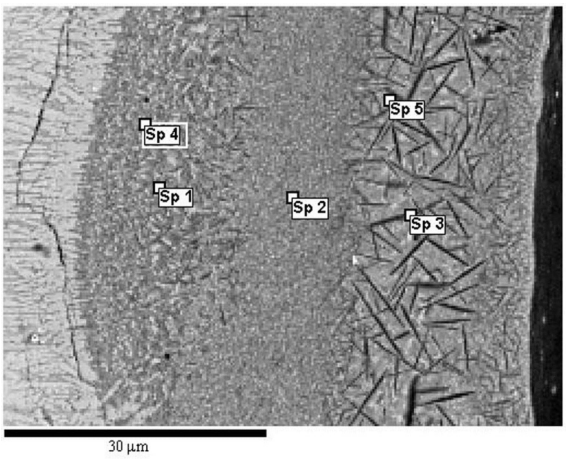

Fig. 5. Microstructure of the cross-section of a ESA coating AlB_{12}-50 wt.% Al on Steel 45 with elemental analysis (substrate is on the left).

reported the formation of the $Al_{13}Fe_4$ phase with a needle-like or angular shape.

The microstructure of the cross-section of a ESA coating with elemental analysis at separate points is shown in Fig. 5 and Table 4. The coating thickness is ~ 53 μm. The microhardness of the layer is H_μ ~ 10 GPa, which can be explained by the essential contribution of intermetallic phases $Al_{13}Fe_4$, AlFe, $AlFe_3$. For example, the hardness of the $Al_{13}Fe_4$ phase is $HV_{0.5}$ 850–1090 [28]. It should also be noted that the $AlFeO_3$ compound has also a high hardness HV 1650–1700 [29]. So, the presence of such phases results in decreasing (in 2.7 times) the weight wear of the ESA coated specimen when compared to the uncoated one (Fig. 6). The friction coefficient $f = 0.37$.

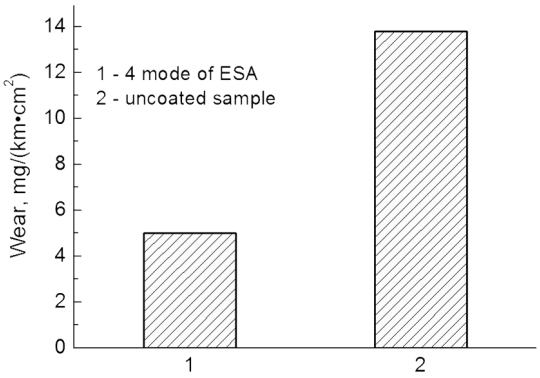

Fig. 6. Wear rate of a ESA coating AlB_{12}-50 wt.% Al on Steel 45.

Table 4. Elemental analysis of the cross-section of a ESA coating AlB_{12}-50 wt.% Al (Fig. 5)

Spectrum (probable phase)	Element, wt.%			Total
	B	Al	Fe	
1 (Fe_3Al)	1.89	13.74	84.37	100.00
2 (Fe_3Al)	2.01	13.81	84.18	100.00
3 ($Al_{13}Fe_4$)	1.25	60.64	38.11	100.00
4 (FeAl)	1.72	31.32	66.96	100.00
5 ($Al_{13}Fe_4$)	1.93	59.36	33.72	100.00

4. Conclusions

The process of the formation of ESA coatings of the AlB_{12}-50 wt.% Al composite on the Steel 45 has been studied. Based on the analysis of the kinetic dependences of mass transfer, the optimal processing mode (mode 4, $E = 0.61$ J) was determined. This is characterized by rather high values of the total cathode mass gain and mass transfer coefficient for the first minutes of alloying. The ESA coating has a thickness of h ~ 53 μm and microhardness H_μ ~ 10 GPa. The ESA treatment contributes in increasing the wear resistance of Steel 45 due to the formation of intermetallic phases in the coating structure.

The AlB_{12}–Al system turned out to be promising from the point of view of its possible application in ESA treatment of steels.

References

1. P.A.Vityaz', A.F.Il'yushchenko, A.I.Shevtsov, Fundamentals of Applying of Wear-, Corrosion-resistant and Heat-shielding Coatings, Bel. Nauka, Minsk (2006) [in Russian].
2. A.V.Bely, A.S.Kalinichenko, A.G.Devoino et al., Engineering of Surfaces of Structural Ma-

terials Using Plasma and Beam Technologies, Bel. Nauka, Minsk (2017) [in Russian].
3. Surface Modification to Improve Properties of Materials, Special Issue Editor: Miran Mozetic, MDPI, Basel, Beijing, Wuhan, Barcelona, Belgrade (2019).
4. Yu.V.Shcherbakov, A.M.Kalifulin, Modern Methods of Restoring and Hardening of Details, Prokrost, Perm (2018) [in Russian].
5. B.Fotovvati, N.Namdari, A.Dehghanghadikolaei, (*J. Manuf. Mater. Process.*, **3**, 28 (2019). https://doi.org/10.3390/jmmp3010028.
6. A.E.Gitlevich, V.V.Mikhailov, N.Ya.Parkansky et al., Electrospark Alloying of Metal Surfaces, Stiinta, Chisinau (1985) [in Russian].
7. A.D.Verkhoturov, I.A.Podchernyaeva, L.F.Pryadko et al., Electrode Materials for Electrospark Alloying, Nauka, Moscow (1988) [in Russian].
8. A.D.Verkhoturov, S.V.Nikolenko, *Strength. Technol. Coat.*, **2**, 13 (2010).
9. M.S.Storozhenko, O.P.Umanskyi, V.B.Tarelnyk et al., *Powder Metall. Met. Ceram.*, **59**, 330 (2020). https://doi.org/10.1007/s11106-020-00166-1
10. O.O.Vasiliev, V.B.Muratov, T.I.Duda, Physics and Chemistry of Solid State, **18**, 358 (2017). https://doi.org/10.15330/pcss.18.3.358-364
11. P.S.Kisly, V.A.Neronov, T.A.Prikhna et al., Aluminum Borides, Nauk. Dumka, Kiev (1990) [in Russian].
12. UA Patent 107193 (2016).
13. UA Patent 107259 (2016).
14. G.N.Dulnev, Yu.P.Zarichnyak, Thermal Conductivity of Mixtures and Composite Materials, Energiya, Leningrad (1974) [in Russian].
15. L.S.Palatnik, *Dokl. Acad. Nauk SSSR*, **LXXXIX**, 455 (1953).
16. O.S.Manakova, A.E.Kudryashov, E.A.Levashov, *Surf. Eng. Appl. Elect.*, **51**, 413 (2015). doi.org/ 10.3103/S1068375515050117
17. V.G.Sorokin, A.V.Volosnikova, S.A.Vyatkin et al., Brands of Steels and Alloys, Mashinostroenie, Moscow (1989) [in Russian].
18. thermalinfo.ru
19. K.Guthmann, *Stahl und Eisen*, **71**, 399 (1951).
20. V.S.Kovalenko, A.D.Verkhoturov, L.F.Golovko et al., Laser and Electroerosion Hardening of Materials, Nauka, Moscow (1986) [in Russian].
21. T.Atoda, I.Higashi, M.Kobayashi, *Sci. Pap. Inst. Phys. Chem. Res.*, **61**, 92 (1967).
22. S.Okada, T.Atoda, *J. of the Ceram. Soc. Jap.*, **88**, 547 (1980).
23. G.Will, *Z. Kristallogr.*, **128**, 156 (1969).
24. S.A.Pyachin, A.A.Burkov, *Surf. Eng. Appl. Elect.*, **51**, 118 (2015). https://doi.org/10.3103/S1068375515020131
25. V.F.Mazanko, D.S.Gertsriken, V.M.Mironov et al., in: Proc. XI Int. Conf. "Interaction of Radiation with Solids", Minsk, Belarus (2015), p.240.
26. S.Frangini, A.Masci, *Surf. Coat. Technol.*, **184**, 31 (2004). https://doi.org/10.1016/j.surfcoat.2003.10.050
27. Jian Gu, Sasa Gu, Lihong Hue et al., *Mater. Sci. & Eng. A*, **558**, 684 (2012). https://doi.org/10.1016/j.msea.2012.08.076
28. M.Windmann, A.Rottger, I.Hahn et al., *Surf. Coat. Technol.*, **321**, 321 (2017). https://doi.org/10.1016/j.surfcoat.2017.04.075
29. L.V.Koroleva, in: Recent Advances in Abrasives Research, ed. by Ing. Dirk Bahre, PhD, Nova Science Publishers Inc., New York, USA (2013), p.173.